

Novel Half-Bridge Resonant Converter Topology Realized by Adjusting Transformer Parameters

Chandan Chakraborty, *Senior Member, IEEE*, Muneaki Ishida, *Member, IEEE*, and Yoichi Hori, *Senior Member, IEEE*

Abstract—This paper shows a new direction as to how the transformer parameters may be best utilized and presents the performance and control of novel dc/dc and ac/dc converter topologies. All three inductances of a transformer have been utilized to realize a CL^3 topology having excellent characteristics and requiring no external inductor. For half-bridge topology, the capacitor used for the purpose of input voltage splitting also serves as the resonating capacitor. Thus, in the half-bridge version, the topology is realized only with a specially designed transformer and no other external components. A laboratory setup is produced and experiments conducted for dc/dc and ac/dc applications. A new design procedure and control technique for the converters are also presented. These topologies are very promising in small-power applications.

Index Terms—Frequency control, half-bridge topology, resonant dc/dc converter, resonant rectifier, transformer magnetics.

I. INTRODUCTION

IN POWER CONVERTER applications where input–output ohmic isolation is mandatory or preferred, a transformer is used and, to reduce the overall size of the converter, the switching frequency is stepped up. For hard-switched converters, an increase in operating frequency results in increased switching losses. However, due to the advantages of zero-voltage switching (ZVS) and/or zero-current switching (ZCS), the resonant converter may be designed to operate at a very high frequency, maintaining high efficiency [1]–[26].

Depending on the topological configurations, resonant converters exhibit a wide range of characteristics. For the voltage-fed network, the basic two-element topologies have their pros and cons and, to improve upon the same, multi-element structures are investigated [3]–[10]. Also, after Steigerwald [3] explained the advantages (i.e., ZVS turn-on and almost loss-free turn-off) to operate a resonant converter in the lagging power-factor mode, operation in this mode has become a standard practice. Multi-element topology offers more variations in characteristics but increases size and cost. Interestingly, transformer-coupled converters may be configured around the transformer by properly taking into account the transformer parameters [11]–[13]. In this context, this paper shows a new direction as to how the transformer parameters

may be best utilized and presents the performance and control of novel dc/dc and ac/dc converter topologies.

II. CHARACTERISTICS OF MULTI-ELEMENT RESONANT CONVERTER TOPOLOGIES

The voltage-fed two-element L – C resonant converter may have two basic variations: 1) the series resonant converter (SRC) and 2) the parallel resonant converter (PRC). The SRC offers good part-load efficiency but at the cost of poor voltage controllability at lower load. With the increase of the load resistance, “selectivity” (change in gain for unit change in frequency ratio) of the network decreases, and at no load the SRC loses all its selectivity (the gain versus frequency-ratio characteristics being a flat line). Therefore, controlling such converter through frequency regulation, which is highly recommended for the half-bridge topology, is not possible. On the other hand, the PRC offers excellent voltage controllability but at the cost of poor part-load efficiency. A compromise of these two topologies results in the LCC series-parallel network. A detailed discussion on this topic is available in [3].

Further investigation on multi-element resonant topologies unearthed all possible combinations of three-element [6], [7] and four-element networks [7]. The available ranges of characteristics for such converters are very rich. However, inclusion of each additional element causes a major penalty of additional losses, size, and cost for the converter. This is why the four-element converter topologies are, so far, not very popular. Among the three-element topologies, the LCC converter is widely investigated, however, this particular topology has the following major drawbacks.

- 1) The topology requires greater range of frequency variation if controlled by changing the operating frequency of the converter. Therefore, the converter elements (including switching devices) can not be best utilized,
- 2) When operated in a wide load range (for example, full load to no load), there is the possibility that the converter enters into the leading power-factor mode, if proper care is not taken by detecting the phase of the current or through a special type of control scheme [16]–[20].

However, the converter has the advantage of simplicity requiring only an extra capacitor. In the half-bridge version, the voltage-splitting capacitor may be used as the series capacitor. Therefore, in a half-bridge LCC converter, the topology requires only the parallel capacitor as the additional element. Full-bridge LCC topologies may be controlled by pulsewidth modulation and/or frequency control [14], [17]. However, for small-power applications, the requirement of four active devices prohibits the use of

Manuscript received December 10, 2000; revised August 8, 2001. Abstract published on the Internet December 5, 2001. This work was supported by Monbusho and the Japan Society for the Promotion of Science.

C. Chakraborty and Y. Hori are with the Department of Electrical Engineering, The University of Tokyo, Tokyo 113-8656, Japan (e-mail: chandan@hori.t.u-tokyo.ac.jp; hori@hori.t.u-tokyo.ac.jp).

M. Ishida is with the Department of Electrical & Electronic Engineering, Mie University, Tsu 514-8507, Japan (e-mail: ishida@ishida.elec.mie-u.ac.jp).

Publisher Item Identifier S 0278-0046(02)00913-9.

such converter in most cases. In [10], the authors have reported a *CLL* topology with suitable characteristics. The major attractions of this topology are as follows.

- 1) It is very suitable to operate in the lagging power-factor mode. In this mode, the gain versus frequency-ratio characteristic being monotonic, the increase in gain with the increase in load resistance may be compensated by a corresponding increase in operating frequency,
- 2) The topology exhibits high-pass characteristics. Thus, the dc voltage (if any) produced due to the inverter ON-OFF switching time mismatch would be absorbed in the series capacitor,
- 3) The unique formation of the network gives rise to the possibility of utilizing the transformer parameters as the converter components for the transformer-coupled network.

However, compared to the *LCC* network, the *CLL* topology has the demerit of requiring an additional inductor (which makes the converter size bigger). Therefore, searching for a prospective topology which will offer excellent performance with minimum penalty in converter size, efficiency, and cost still remained a challenge.

With the motivation of reducing the number of switches, the half-bridge topologies have definite advantages. Therefore, studies of corresponding full-bridge topologies, which are simple extensions of the present work, are kept outside the scope of this investigation. It is only for the transformer-coupled converter that the reduction of transformer size becomes an issue, and it is in this area that the authors believe that the resonant converters have a competitive edge over the existing switch-mode topologies. Therefore, the present work deals with the realization of a resonant topology with minimum additional components by best utilizing the parameters of a specially designed transformer.

III. DEVELOPMENT OF THE PROPOSED SYSTEM

The simplified transformer equivalent circuit (ignoring the core loss) is shown in Fig. 1. Usually, for a normal transformer the leakage (primary and secondary) inductances are too small and the magnetizing inductance is too large and, hence, are not suitable to replace any of the inductances used to form the resonant topology. In earlier publications, the authors presented a *CLL* topology which is ideal to operate in the lagging power factor mode and offers excellent characteristics [10]. However, the network requires two inductors and, therefore, is bigger in size. Interestingly, if a capacitor is only added to the transformer equivalent circuit, a *CL³* type of topology results and if the primary leakage can be made negligible, then the topology becomes the *CLL*. Due to the presence of L_1 , the *CL³* becomes better compared to the *CLL* in controlling the output voltage by controlling the operating frequency at lower load and/or no load [23]. This paper shows that the *CL³* topology is also equally suitable to operate in the lagging power-factor mode and proposes a simple realization of the network for both dc/dc and ac/dc applications.

Fig. 2 shows the dc/dc and ac/dc resonant converter topologies that use a specially designed transformer (*ST*). The special transformer offers three adjustable inductances. The voltage-

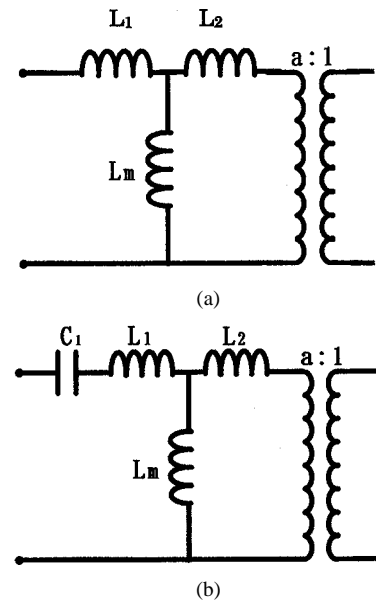


Fig. 1. Development of the proposed topology. (a) Simplified equivalent circuit of the transformer. (b) *CL³* topology realized by a specially designed transformer with only a capacitor added.

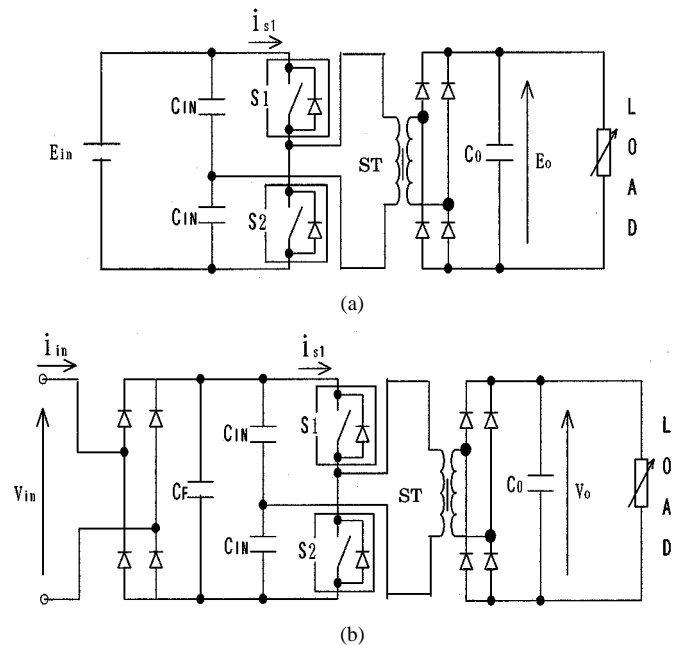


Fig. 2. Proposed converter topologies (*ST*: special transformer). (a) DC/DC converter. (b) AC/DC converter.

splitting capacitors are also used as the capacitor ($C_1 = 2C_{IN}$) in the resonant network. A half-bridge inverter is used to reduce the device count. In the case of the ac/dc converter, an additional capacitor C_F is used to filter out the high-frequency current components generated due to the inverter switching. In both systems, although full-bridge diode-rectifiers are used, full bridges may be replaced by corresponding half bridges to further reduce the number of devices.

The special transformer with higher leakage and lower magnetizing inductance may be realized in a number of ways. A simpler one utilizing an E-I-type ferrite core, readily available in our laboratory, is produced as shown in Fig. 3. Litz wire is used to reduce

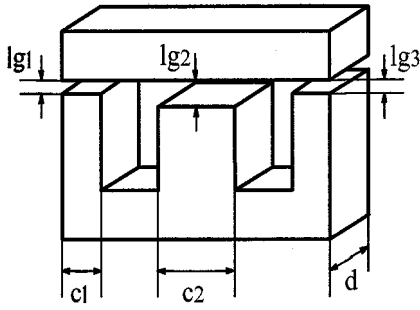


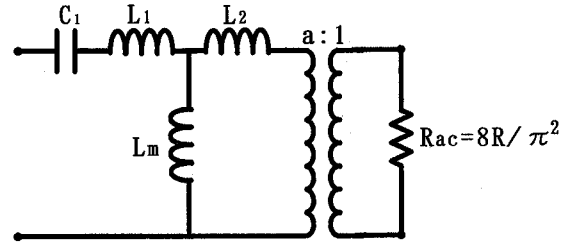
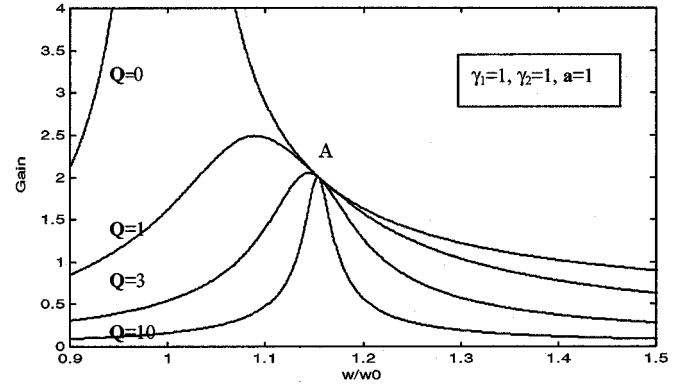
Fig. 3. Transformer core details.

the skin effect. Windings are placed on the outer limbs with primary on one side and secondary on the other. This configuration produces enough leakage for both the primary and the secondary. Inductances may be adjusted through the air-gap lengths. For simplicity, lg_1 and lg_3 are kept equal in this study. While this is one of the simplest winding placements possible, further investigation in the direction of: 1) better winding placement and 2) selection of core structure and core material, particularly from the point of view of ease of fabrication, cost, and efficiency are required. The authors' motivation in this paper is to show how all of the transformer parameters may be best utilized, giving rise to attractive resonant converter topologies requiring no additional elements. The ferrite core is used mainly because of the availability of wide range of shapes and also due to the cost and weight advantage over Permalloy [24]. In the present study with relatively low operating frequency (in the range of 20–50 kHz), the effect of winding capacitance is neglected, however, the same is to be considered when designing converters at higher operating frequency (i.e., at 1MHz and beyond).

IV. CONVERTER PERFORMANCE

Due to specific advantages [3], the converter is operated only in the lagging power-factor mode and at rated load the current phase lag is reduced to minimum to consume minimum voltamperes to supply the rated power (watts). AC sinusoidal analysis has been carried out to bring out the important features of the network. Also, converter components and devices are considered to be ideal. The simplified equivalent circuit is shown in Fig. 4. The expression for the converter ac gain may be derived as (1), shown at the bottom of the page, where

$$\begin{aligned} x &= \frac{\omega}{\omega_0} \\ \mathbf{L}_1 &= \gamma_1 \mathbf{L}_m \\ \mathbf{L}_2 &= \gamma_2 \mathbf{L}_m \\ \omega_0 &= \frac{1}{\sqrt{(1 + \gamma_1) \mathbf{L}_m C_1}} \\ \mathbf{Q} &= \frac{\omega_0 \mathbf{L}_m (1 + \gamma_1)}{\mathbf{R}} = \frac{1}{\omega_0 C_1 \mathbf{R}} \end{aligned}$$

Fig. 4. Simplified equivalent circuit (\mathbf{R} = load resistance).Fig. 5. \mathbf{M} versus ω/ω_0 characteristic for different \mathbf{Q} .

Therefore, the converter gain at no load ($\mathbf{M} = \mathbf{M}_0$) becomes

$$\mathbf{M}_0 = \frac{1}{a(1 + \gamma_1) \left(1 - \frac{1}{x^2}\right)}. \quad (2)$$

The converter gain (\mathbf{M}) will become load independent if

$$x = \sqrt{\frac{(1 + \gamma_1)(1 + \gamma_2)}{\gamma_1 + \gamma_1 \gamma_2 + \gamma_2}}. \quad (3)$$

Fig. 5 shows the converter-gain (\mathbf{M}) versus frequency-ratio ($= \omega/\omega_0$) characteristic for $\gamma_1 (= \mathbf{L}_1/\mathbf{L}_m) = 1.0$ and $\gamma_2 (= \mathbf{L}_2/\mathbf{L}_m) = 1.0$ and for different magnitudes of \mathbf{Q} ($= 0, 1, 3,$ and 10). The curve corresponding to $\mathbf{Q} = 0$ represents the no-load characteristics. The no-load gain (\mathbf{M}_0) depends on the frequency ratio, transformer turns ratio (\mathbf{a}), and γ_1 . From Fig. 5, it has been observed that at the point “A” (determined by the frequency ratio and γ s), the converter exhibits the load-independent feature. Therefore, if the converter is designed to operate at or near the load-independent point, then the output voltage can be controlled by a small change in operating frequency. This allows better utilization of the converter components. The load-independent points are decided by (3). Hence, in the lagging power-factor mode, the converter may

$$\mathbf{M} = \frac{1}{a \sqrt{\left\{ (1 + \gamma_1) \left(1 - \frac{1}{x^2}\right) \right\}^2 + \frac{\pi^4 \mathbf{Q}^2}{64 a^4} \left\{ \left(\frac{\gamma_1 + \gamma_2 (1 + \gamma_1)}{(1 + \gamma_1)} \right) x - \left(\frac{1 + \gamma_2}{x} \right) \right\}^2}} \quad (1)$$

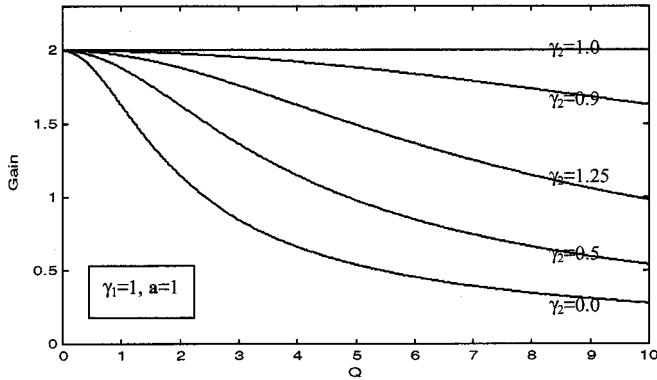


Fig. 6. M versus Q characteristic for different γ_2 .

be operated at any point on the no-load characteristic with the load-independent feature remaining valid if the (2) and (3) are always satisfied. However, if the operating frequency moves toward left the no-load gain and “selectivity” of the converter increase and the part-load efficiency decreases because the current through the $C_1-L_1-L_m$ path increases. Interestingly, if a converter is designed to operate at point “A” at rated load, then with the decrease in load current, the converter automatically enters in the lagging power-factor mode. Thus, in the full range of operation, the converter remains in the lagging power-factor mode, dispensing with the need of a device snubber [3]. To compensate for the variation in input voltage, the converter needs to be designed corresponding to the minimum input voltage and maximum load current, and for all other loading conditions, the frequency may be controlled to keep output voltage constant. A typical load characteristic of the converter is shown in Fig. 6. The data correspond to point “A” of Fig. 5 with $\omega/\omega_0 = 1.1547$ and shows the effect of secondary leakage (in terms of γ_2). It is again clear that only a specific amount of leakage provides best operation. Thus, the parameters a , γ_1 , and ω/ω_0 offer control over no-load performance whereas the load characteristic is decided by γ_2 together with γ_1 , a , and ω/ω_0 as decided from the no-load requirement. This explains the requirement of proper attention to all the existing inductances of the special transformer (ST) to obtain optimum performance.

A new variable β has been introduced for the purpose of design. For a transformer with unity turns ratio, β is the ratio of currents flowing through the transformer primary in the case of no load to that flowing through the secondary in the case of full -load. In general, for a transformer with any turns ratio, β is defined by the ratio of both of these currents referred to the primary side of the transformer. Thus, for simplicity, assuming $\gamma = \gamma_1 = \gamma_2$ and knowing β , M , ω , a , and R , the converter components may be found from the following equations:

$$L_m = \left(\frac{8}{\pi^2}\right) a^2 \frac{R}{\omega\beta} \quad (4)$$

$$C_1 = 2C_{IN} = \frac{aM}{(a^2M^2 - 1)\omega^2L_m} \quad (5)$$

$$L_1 = L_2 = \left(\frac{8}{\pi^2}\right) \frac{a^2(aM - 1)R}{\omega\beta} \quad (6)$$

As β decides the current flowing through the converter at no load, it therefore has a direct influence on the efficiency of the

converter at no load and lower load. Details of the influence of β and ω on the converter design are available in [21] and [23], and (4)–(6) also contain the turns ratio (a) of the converter as another important variable. It is obvious that the same converter gain is possible with various combinations of a , γ , and frequency ratio ($x = \omega/\omega_0$) [23]. While β may be selected properly to have desirable efficiency, the turns ratio may be adjusted to have optimum size. Thus, a proper selection of β and a will offer overall good performance of the converter. Now, considering a to be an independent variable, the size of the converter may be optimized if the following condition is satisfied [23]:

$$\frac{d}{da} \{L_1 I_{L1}^2 + L_m I_{Lm}^2 + L_2 I_{L2}^2\} = 0. \quad (7)$$

Using (4), (6), and on algebraic simplification, an expression for the optimum magnitude of a may be derived from (7) as

$$a = \sqrt{\frac{\omega L_m}{10R_{ac}^2} \left\{ \sqrt{(9\omega^2 L_m^2 M^4 + 20R_{ac}^2)} - 3\omega L_m M^2 \right\}} \quad (8)$$

where

$$R_{ac} = \left(\frac{8}{\pi^2}\right) R.$$

Finally, the inductors (L_1 , L_2 , and L_m) are to be defined in terms of the core dimension of the special transformer. For simplification: 1) the reluctance of the core is neglected compared to that of the air gap and 2) the fringing flux around the edges is taken into account by assuming that the region of uniform flux density extends outward from each of the gap edges by a length equal to half of the gap length [11], [23]. With reference to the core dimensions as shown in Fig. 3, the following expressions may be derived for L_1 , L_2 , and L_m :

$$L_1 = L_2 = \frac{N_1^2 \mu_0 k_g (c_{1g} d_g) (c_{2gg} d_{gg})}{l_g (2c_{1g} d_g + k_g c_{2gg} d_{gg})} \quad (9)$$

$$L_m = \frac{N_1^2 \mu_0 (c_{1g} d_g)^2}{l_g (2c_{1g} d_g + k_g c_{2gg} d_{gg})} \quad (10)$$

where

$$l_{g1} = l_{g3} = l_g$$

$$k_g = \frac{l_{g1}}{l_{g2}}$$

$$c_{1g} = c_1 + l_g$$

$$c_{2gg} = c_2 + l_{g2}$$

$$d_g = d + l_g$$

$$d_{gg} = d + l_{g2}.$$

The inductances are referred to primary.

For ac/dc applications, the converter may be thought of as a diode-rectifier-fed dc/dc converter. The input ac voltage is rectified and the unfiltered dc voltage is applied to the dc/dc converter. As the switching frequency (f) of the inverter is quite high compared to that of the power frequency, the voltage applied to the inverter during a switching time period ($T = 1/f$) appears to be almost dc and, thus, the converter components may

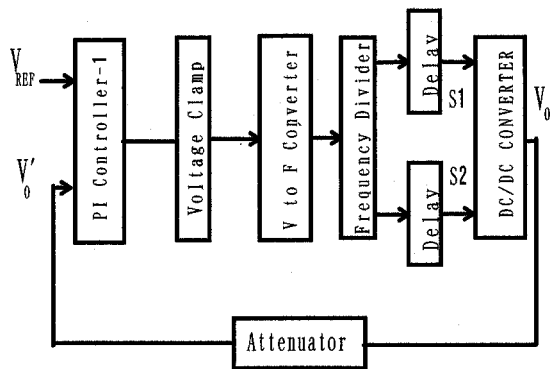


Fig. 7. Control schematics for dc/dc converter.

be designed corresponding to the maximum power transfer condition [14], [17].

V. CONVERTER CONTROL

The converter control aspects have been developed with the motivation of keeping output voltage constant despite change of load and variation in input voltage for the dc/dc converter. For the ac/dc converter, the additional requirement is set to have a better input-current waveform. Investigation and improvement of the converter dynamic response [25], [26] are kept outside the scope of the present study.

A. For DC/DC Converter

A proportional plus integral (PI) controller-fed voltage-controlled-oscillator (VCO)-type control scheme is found suitable for such a type of converter. The controller senses the output voltage, compares the same with a reference, generating an error signal, which is processed by the PI controller. The PI controller output is fed to the VCO to generate the necessary gate-drive signals of the insulated gate bipolar transistors (IGBTs). Details of the control blocks are shown in Fig. 7. It is to be noted that when operated at or near point “A” (Fig. 5), the network requires short-circuit protection. As the voltage across the capacitor increases monotonically with the increase of the load, the capacitor voltage is sensed, compared with a reference and, if exceeded, the gate drive of the IGBT is withdrawn. This has the advantage of requiring no current sensor for safe operation of the system.

B. For AC/DC Converter

The controller in AC/DC converter has to serve the dual purpose of output-voltage-control and input-current-shaping. The output voltage is controlled in the same way as of the DC/DC converter. However, depending on the technique of the input-current-shaping, two new control strategies have been developed as shown in Figs. 8 and 9

To develop Control Scheme 1, the converter is initially operated only with the voltage control hardware and the input current of the converter is observed. A sample nature of the converter input current is shown in Fig. 10. The desired waveform being a sine wave (shown with broken lines in the figure), the waveform from the experiment shows that the converter draws less current near the zero crossing and more current near the

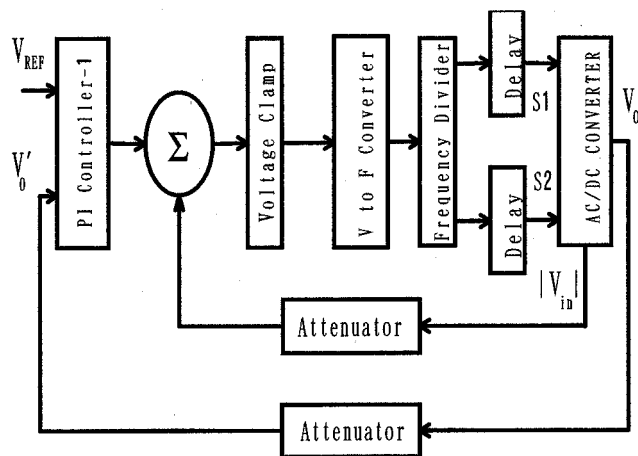


Fig. 8. Control Scheme 1.

voltage peak. As the converter is operated always in the lagging power-factor mode, a monotonic gain versus frequency-ratio relation exists, which may be exploited to improve the waveform of the input current of the converter. The technique is through fixed-frequency modulation. Operating frequency is reduced near the zero crossing and increased near the voltage peak. Reduction in frequency would bring the operating point toward the corresponding resonating frequency, reducing the equivalent impedance. Therefore, under such circumstance the converter draws more current from the input. With similar logic, when the operating frequency is moved away from the resonating frequency, the corresponding impedance increases, reducing the corresponding current intake from the supply. This is achieved simply by adding a voltage, proportional to the rectified source voltage, to the output of the PI controller as shown in Fig. 8. This control scheme is very simple and does not require a current sensor.

To further improve the converter input current, use of a current sensor is recommended. This is presented in Control Scheme 2. A current sensor and associated circuitry are added to Control Scheme 1. The input current is sensed and compared with a reference, generating an error signal, which is processed by a PI controller. The output of the PI controllers drives the VCO. The details of the scheme are shown in Fig. 9. Two PI controllers are used, as shown.

VI. EXPERIMENTAL RESULTS

A. For DC/DC Converter

An experimental prototype of the converter has been fabricated in the laboratory. A 48-V input and 24-V, 1-A output dc/dc converter application has been considered. A transformer with “1:1” turns ratio is produced with $L_1 = 65.8 \mu\text{H}$, $L_2 = 64.6 \mu\text{H}$, and $L_m = 54 \mu\text{H}$. The corresponding gap lengths are $l_{g1} = l_{g3} = 0.25 \text{ mm}$ and $l_{g2} = 0.4 \text{ mm}$. Thus, the middle leg of the E-core is cut only for a 0.15-mm thickness. A capacitor $C_{IN} = 0.11 \mu\text{F}$ has been used. Operating frequency is considered to be around 35 kHz. The controller is realized and found to perform satisfactorily. Fig. 11 shows the waveform for full-load and half-load conditions. From full load to half load, a frequency increment of only 1.01 kHz is required to control the output

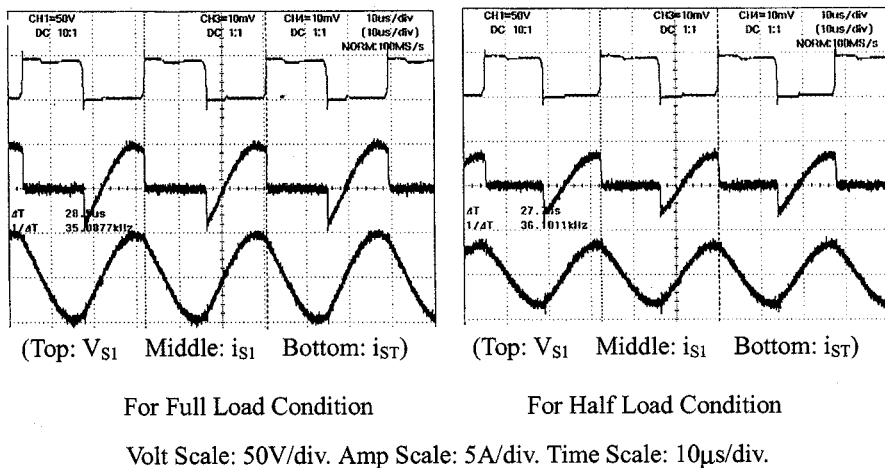


Fig. 11. Experimental waveforms for dc/dc converter.

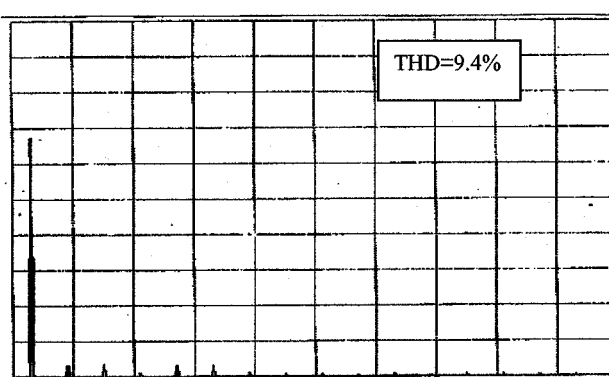
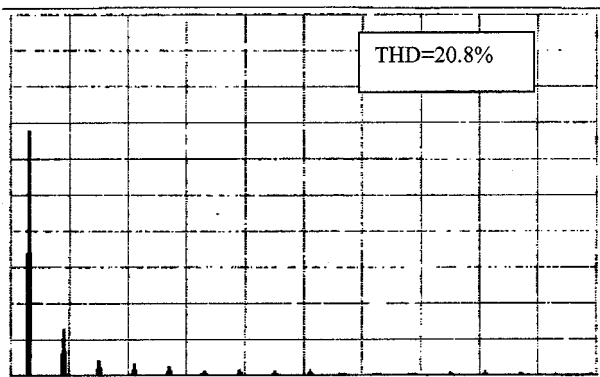
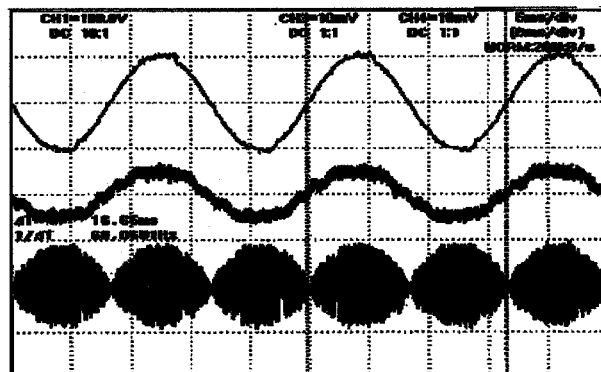
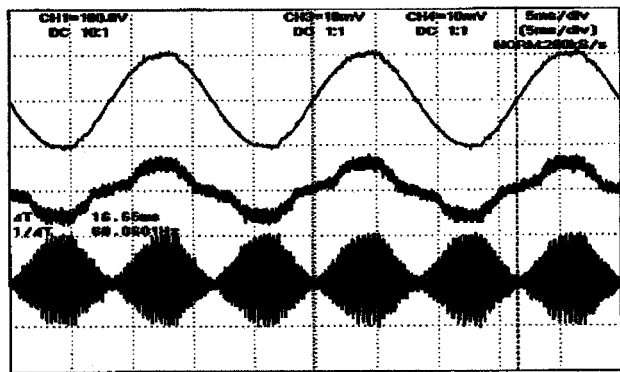


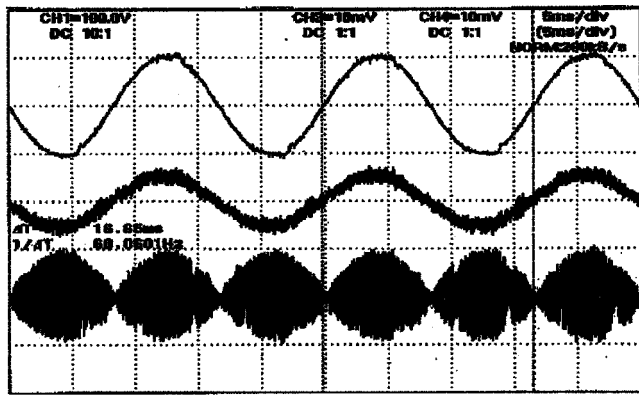
Fig. 12. Experimental waveforms with no current control. (a) Voltage and current waveforms. (b) Harmonic spectrum of converter input current (scale: 1 V = 2.2 A rms).

Fig. 13. Experimental waveforms with Control Scheme 1 in operation. (a) Voltage and current waveforms. (b) Harmonic spectrum of converter input current (scale: 1 V = 2.2 A rms).

VII. CONCLUSIONS

This paper has introduced a new way to realize transformer-coupled resonant converters by properly utilizing the

transformer parameters. For such purpose, the transformer is specially designed with increased leakage and reduced magnetizing inductances. Adding only a capacitor, a series-parallel

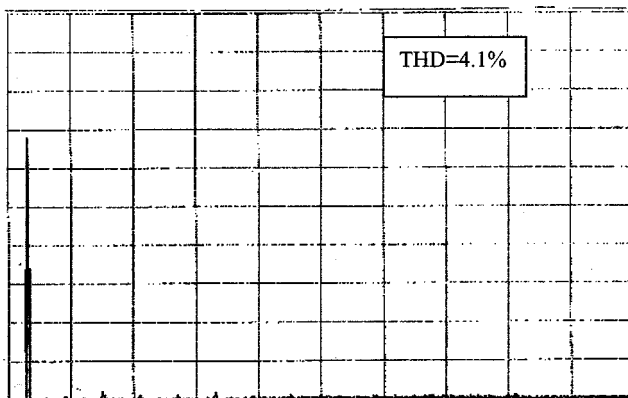


(Top: V_{in} Middle: i_{in} Bottom: i_{s1})

Scale: Top=100V/div. Middle=5A/div. Bottom=10A/div.

Time Scale: 5ms/div.

(a)



(Horizontal Full Range=0-2kHz Vertical Full Range=0-1V)

(b)

Fig. 14. Experimental waveforms with Control Scheme 2 in operation. (a) Voltage and current waveforms. (b) Harmonic spectrum of converter input current (scale: 1 V = 2.2 A rms).

CL^3 topology is formed, which is very suitable to operate in the lagging power-factor mode, dispensing with the need for a device snubber. Also, proper design of such converters will enable the same to operate with minimum variation in operating frequency despite change in operating conditions. Several aspects for dc/dc and ac/dc converters have been discussed. Novel control methods have been reported in the case of ac/dc converters, which will keep the output voltage constant and also shape the input current of the converter. Laboratory prototypes of the dc/dc and ac/dc converters have been realized and excellent performance has been confirmed. The proposed control method for the ac/dc converter yields a THD as low as 4.1% for the input current of the converter while smoothly controlling the converter output voltage. These types of converters are very promising, particularly in the small output range.

ACKNOWLEDGMENT

The authors acknowledge the reviewers' comments, which helped to improve the content of the paper. Support from

Prof. T. Hori of Mie University, Japan, and from The University of Tokyo (Japan), Mie University (Japan), and Jadavpur University (India) is also acknowledged.

REFERENCES

- [1] V. T. Ranganathan, P. D. Ziogas, and V. R. Stefanovic, "A regulated dc-dc voltage source converter using a high frequency link," *IEEE Trans. Ind. Applicat.*, vol. 18, pp. 279–287, May/June 1982.
- [2] R. Oruganti and F. C. Lee, "Resonant power processors, Part I-state plane analysis," *IEEE Trans. Ind. Applicat.*, vol. IA-21, pp. 1453–1960, Nov./Dec. 1985.
- [3] R. L. Steigerwald, "A comparison of half-bridge resonant converter topologies," *IEEE Trans. Power Electron.*, vol. 3, pp. 174–182, Apr. 1988.
- [4] A. K. S. Bhat and M. M. Swami, "Analysis of parallel resonant converter operating above resonance," *IEEE Trans. Aerosp. Electron. Syst.*, vol. 25, pp. 449–458, July 1989.
- [5] T. Ninomiya, M. Nakahara, T. Higashi, and K. Harada, "A unified analysis of resonant converters," *IEEE Trans. Power Electron.*, vol. 6, pp. 260–270, Mar. 1991.
- [6] R. P. Severns, "Topologies of three-element converters," *IEEE Trans. Power Electron.*, vol. 7, pp. 89–98, Jan. 1992.
- [7] I. Batarseh, "Resonant converter topologies with three and four energy storage elements," *IEEE Trans. Power Electron.*, vol. 9, pp. 64–73, Jan. 1994.
- [8] S. Hamada and M. Nakaoka, "Analysis and design of saturable reactor assisted soft-switching DC-DC converter," *IEEE Trans. Power Electron.*, vol. 9, pp. 309–317, May 1994.
- [9] J. H. Cheng and A. F. Witulski, "Analytic solution for LLC parallel resonant converter simplify use of two- and three-element converters," *IEEE Trans. Power Electron.*, vol. 13, pp. 235–243, Mar. 1998.
- [10] C. Chakraborty, M. Ishida, and T. Hori, "A half bridge CLL resonant DC/DC converter," *Trans. Inst. Elect. Eng. Jpn.*, vol. 119-D, no. 12, pp. 1558–1559, 1999.
- [11] H. A. Kojori, J. D. Lavers, and S. B. Dewan, "State plane analysis of a resonant dc-dc converter incorporating integrated magnetics," *IEEE Trans. Magn.*, vol. 24, pp. 2898–2900, Nov. 1988.
- [12] R. Farrington, M. M. Jovanovic, and F. C. Lee, "A new family of isolated converters that uses the magnetizing inductance of the transformer to achieve zero-voltage switching," *IEEE Trans. Power Electron.*, vol. 8, pp. 535–545, Oct. 1993.
- [13] H. J. Jiang, G. Maggetto, and P. Lataire, "Steady-state analysis of the series resonant DC-DC converter in conjunction with loosely coupled transformer-above resonance operation," *IEEE Trans. Power Electron.*, vol. 14, pp. 469–480, May 1999.
- [14] M. J. Schutten, R. L. Steigerwald, and M. H. Kheraluwala, "Characteristics of load resonant converters operated in a high-power factor mode," *IEEE Trans. Power Electron.*, vol. 7, pp. 304–314, Mar. 1992.
- [15] W. Sulistyono and P. Enjeti, "A series resonant AC-to-DC rectifier with high-frequency isolation," *IEEE Trans. Power Electron.*, vol. 10, pp. 784–790, Nov. 1995.
- [16] J. Hong, D. Maksimovic, R. W. Ericson, and I. Khan, "Half cycle control of the parallel resonant converter operated as a high power factor rectifier," *IEEE Trans. Power Electron.*, vol. 10, pp. 1–8, Jan. 1995.
- [17] V. Belaguli and A. K. S. Bhat, "Operation of the LLC type parallel resonant converter as a low harmonic rectifier," *IEEE Trans. Ind. Electron.*, vol. 46, pp. 288–299, Apr. 1999.
- [18] H. Pinheiro, P. Jain, and G. Joos, "Series-parallel resonant converter in the self-sustained oscillating mode for unity power factor applications," in *Proc. IEEE APEC'97*, 1997, pp. 477–483.
- [19] V. R. Durgesh, A. Muthuramalingam, and V. V. Sastry, "Operation of fixed frequency class-D series-parallel resonant converter on utility line with active control," in *Proc. IEEE APEC'99*, 1999, pp. 375–381.
- [20] S. V. Mollov and A. J. Forsyth, "Analysis, design and resonant current control for a 1-MHz high-power-factor rectifier," *IEEE Trans. Ind. Electron.*, vol. 46, pp. 620–627, June 1999.
- [21] C. Chakraborty, M. Ishida, and T. Hori, "Performance and design of an LCL converter for voltage regulator type applications," *Trans. Inst. Elect. Eng. Jpn.*, vol. 119-D, no. 6, pp. 848–856, 1999.

- [22] C. Chakraborty and M. Ishida, "A low harmonic high power factor half bridge resonant AC/DC converter," *Trans. Inst. Elect. Eng. Jpn.*, vol. 120-D, no. 11, pp. 1328–1334, 2000.
- [23] C. Chakraborty, "Studies on small size high performance resonant power conversion systems," Ph.D. dissertation, Mie University, Tsu, Japan, 2000.
- [24] M. H. Kheraluwala, D. W. Novotny, and D. M. Divan, "Coaxially wound transformers for high-power high-frequency applications," *IEEE Trans. Power Electron.*, vol. 7, pp. 54–62, Jan. 1992.
- [25] M. Hernando, J. Sebastian, P. J. Villegas, and S. Ollero, "Improving dynamic response of power-factor correctors by using series-switching postregulator," *IEEE Trans. Ind. Electron.*, vol. 46, pp. 563–568, June 1999.
- [26] P. J. Villegas, J. Sebastian, M. Hernando, F. Nuno, and J. A. Martinez, "Average current mode control of series-switching post-regulators used in power factor correctors," *IEEE Trans. Power Electron.*, vol. 15, pp. 813–819, Sept. 2000.



Chandan Chakraborty (SM'01) received the B.E. (with Honors) and M.E. degrees from Jadavpur University, Jadavpur, India, in 1987 and 1989, respectively, and Ph.D. degrees from Indian Institute of Technology, Kharagpur, India, and Mie University, Mie, Japan, in 1997 and 2000, respectively, all in electrical engineering.

He is currently with The University of Tokyo, Tokyo, Japan. His fields of interest are power converters, motor control, renewable energy systems, and electric vehicles.

Dr. Chakraborty is a member of the IEEE Industrial Electronics, IEEE Industry Applications, IEEE Power Electronics, and IEEE Power Engineering Societies. He is also a member of the Institute of Engineers (India) and Institute of Electrical Engineers of Japan. He has received the Monbusho and the Japan Society for the Promotion of Science Fellowship Awards from the Japanese Government. He has authored several papers published in IEEE TRANSACTIONS and conference proceedings.



Muneaki Ishida (M'82) was born in Aichi, Japan, in 1952. He received the B.E., M.E., and D.E. degrees in electrical and electronic engineering from Nagoya University, Nagoya, Japan, in 1975, 1977, and 1980, respectively.

He was with the Department of Electrical Engineering, Nagoya University, as a Research Associate from 1980 to 1987. From 1987 to 1996, he was an Associate Professor in the Department of Electrical and Electronic Engineering, Mie University, Tsu, Japan, where, since 1996, he has been a Professor. His research interests include resonant power converters, ac motor drives, and applications of active filters.

Prof. Ishida is a member of the IEEE Industrial Electronics, IEEE Industry Applications, IEEE Power Electronics, and IEEE Power Engineering Societies. He is also a member of the Institute of Electrical Engineers of Japan, Society of Instrument and Control Engineers of Japan, and Japan Society of Mechanical Engineers.



Yoichi Hori (SM'00) received the B.S., M.S., and Ph.D. degrees in electrical engineering from The University of Tokyo, Tokyo, Japan, in 1978, 1980, and 1983, respectively.

In 1983, he joined the Department of Electrical Engineering, The University of Tokyo, as a Research Associate. He later became an Assistant Professor and an Associate Professor. Since 2000, he has been a Professor. During 1991–1992, he was a Visiting Researcher at the University of California, Berkeley. His research fields are control theory and its industrial applications, in particular, to motion control, mechatronics, robotics, power electronics, and electric vehicles.

Prof. Hori is a member of the Institute of Electrical Engineers of Japan, Japan Society of Mechanical Engineers, Society of Instrument and Control Engineers of Japan, Institute of Systems, Control and Information Engineers, Robotic Society of Japan, Japan Society of Simulation Technology, Japan Society of Mechanical Engineers, and Society of Automotive Engineers of Japan.